Earthq Eng & Eng Vib (2009) 8:207-217 **DOI**: 10.1007/s11803-009-9025-4

Emergency assessment of seismic landslide susceptibility: a case study of the 2008 Wenchuan earthquake affected area

Tang Chuan†, Zhu Jing‡ and Liang Jingtao*

State Key Laboratory of Geo-Hazard Prevention, Chengdu University of Technology, Chengdu 610059, China

Abstract: The 8.0 M_w Wenchuan earthquake triggered widespread and large scale landslides in mountainous regions. An approach was used to map and assess landslide susceptibility in a given area. A numerical rating system was applied to five factors that contribute to slope instability. Factors such as lithology, topography, streams and faults have an important influence as event-controlling factors for landslide susceptibility assessment. A final map is provided to show areas of low, medium, and high landslide susceptibility. Areas identified as having high landslide susceptibility were located in the central, northeastern, and far south regions of the study area. The assessment results will help decision makers to select safe sites for emergency placement of refuges and plan for future reconstruction. The maps may also be used as a basis for landslide risk management in the study area.

Keywords: landslide; susceptibility; GIS; Wenchuan earthquake; Qingchuan area

1 Introduction

A strong earthquake occurred on May 12, 2008 with its epicenter located 90 km northwest of Chengdu City in Sichuan Province, China. The magnitude 8.0 on the Richter-scale earthquake was among the strongest that have occurred in relatively densely populated areas in China. The earthquake triggered more than 15,000 landslides in the steep mountainous terrain, in an area of about 50,000 km^2, causing more than 20,000 fatalities (1/4 of the total of fatalities and persons missing due to the earthquake) (Yin, 2009). The coseismic landslides caused major damage to settlements and irrigation waterways, blocked or destroyed highways and bridges, isolated the city of Wenchuan and many other towns, and frustrated rescue and relief efforts. Landslides that occurred close to rivers created 34 large barrier lakes that threatened more residents who lived downstream of these dams. In an emergency field investigation and interpretation of aerial photographs conducted by the State Key Laboratory of Geohazard Prevention (SKLGP) in the area of Qingchuan County after the earthquake, 971 landslides were identified within a 3271 km^2 area. The aim was to develop a set of landslide susceptibility maps for the entire area affected by the Wenchuan earthquake in response to an emergency request from the government of China and local authorities. For this purpose, the area of Qingchuan County was selected as a case study, so the approach used could then be applied to the entire affected area. The emergency maps will help decision makers select safe sites for emergency placement of refuges and plan for future reconstruction. The maps may also be used as a basis for landslide risk management in the study area.

Correspondence to: Tang Chuan, State Key Laboratory of Geo-hazard Prevention, Chengdu University of Technology, Chengdu 610059, China
Tel: +86-028-84077505; Fax: +86-028-84078948
E-mail: tangc707@gmail.com
†Professor; ‡Associate Professor; *Graduate Student

Supported by: Research Foundation of SKLGP; National Natural Science Foundation of China Under Grant No. 40772206; 973 Program Under Grant No.2008CB425801
Received Februry 2, 2009; **Accepted** April 17, 2009

2 Methods

2.1 Study area

This study focused on an area located northeast of the earthquake's epicenter, in Qingchuan County of Sichuan Province. The area was selected because of its moderate-high seismic activity. Three of the aftershocks exceeded magnitude 6, including the largest, which had a magnitude of 6.4. The area is 250 km away from the northern part of Chengdu, with eastern longitude of 104º36′ to 105º38′, and northern latitude of 32º12′ to 32º56′. It is 105 km long from east to west and 96 km long from south to north, covering 3,271 km^2 and accommodating approximately 250,000 people.

The Qingchuan area is underlain by a wide variety of sedimentary and metamorphic rock and unconsolidated sedimentary deposits and exposed strata of Cambrian, Silurian, Devonian, Carboniferous, Triassic, and Jurassic age and Quaternary loose deposits. The rocks include Cambrian metavolcanite, metasandstone and

slate, Silurian phyllite, and Devonian and Carboniferous limestone, Triassic quartzitic sandstone and shale, Jurassic sandy gravel and Sandshale; Quaternary loose deposits are widely distributed in the terraces and alluvial fans. These rocks are typically poorly or moderately indurated, structurally deformed by pervasive folding and faulting, and covered by residual and colluvial soils as much as several meters deep. The geological structure of the study area shows mainly a north-east orientation; the strike of the rock strata shows the same orientation. The Longmenshan fault zone in relation to the 2008 Wenchuan earthquake is just through the study area (Fig. 1). The Longmenshan Fault system is on a steeply northwest-dipping plane comprised of three faults called the Yingxiu-Beichuan, Guanxian-Jiangyou, and Maoxian-Wenchuan Faults. The Yingxiu-Beichuan fault that triggered the Wenchuan earthquake is located just south central of the study area, and is developed as a thrust fault with a NW dipping angle of 60° to 70°. The Guanxian-Jiangyou Fault is far south of the study area. There is another active fault named the Pingwu-Qingchuan Fault located north central to the study area, with a NEE orientation (Fig. 2).

Qingchuan County is located at the transitional belt between the Sichuan Basin and the Western Sichuan Plateau, and is mainly composed of mountainous areas. The northwestern part of the area is characterized by high relief mountains with an elevation of 1800–3837 m; the central part is characterized by medium relief landscape with an elevation of 1200–1800 m; and the southeastern part is low and medium relief mountains with an elevation of 491–1200 m. The highest mountain in the study area is Mt. Dacaoping, with an elevation of 3837 m; and the lowest area is the Qingzhu River near Jinzishan area, with an elevation of 491 m.

The region is drained by the Bailong River and its two tributaries: the Qingzhu and Qiaozhuang Rivers. These three rivers flow very rapidly with discharges of approximately 525, 30, and 40 m^3/s, respectively. The Bailong River flows just through the east corner of the study area with 66 km long. The Qingzhu River, with 124 km long, originates in the northwestern mountainous area, and flows westward forming deep antecedent valleys before flowing southwards along broader valleys to the Bailong River. The Qiaozhuang River enters the study area from the north and flows through Qingchuan City, and then turns east, running into the Beilong River.

The study area is situated in the subtropical humid monsoon climate zone, with an annual average temperature of 13.7 ºC. The annual average precipitation is 1021.7 mm, with the highest amount of annual precipitation being 1780 mm (in 1961). Rainfall is mostly concentrated in the period between June and September, with 80% of the annual precipitation and 90% in the years of highest precipitation (in 1981). From a spatial distribution perspective, the Qingchuan area shows a trend of decreasing precipitation from northwest to southeast.

2.2 Data acquisition

The basic data used in this study included a 20 m

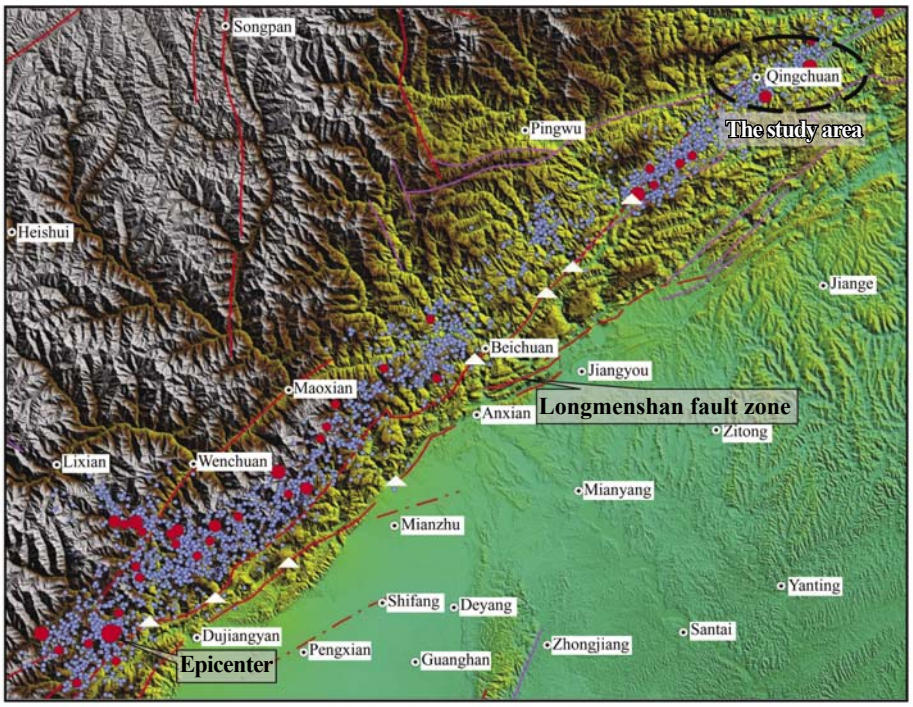

Fig. 1 Map showing the study area and the Longmenshan fault zone

× 20 m grid digital elevation model (DEM), 1:100,000 geologic maps and 1:5000 selected aerial photographs. The geological maps were collected from the China Geological Survey (CGS). Aerial photographs were taken by the Ministry of Land and Resources (MLR) after the occurrence of Wenchuan earthquake. The following landslide susceptibility factor maps were generated:

• Rock type map, indicating the main geological units in the areas. This map was digitized from the existing geological map with a scale of 1:100,000.

• Structural geological map, only showing the location of faults. This map was constructed based on existing geological information and additional fieldwork.

• Slope gradient: This map was generated from the DEM. The DEM was made through the interpolation of contour lines from 15 digitized 1:50,000 toposheets, with a contour interval of 5 meters. The slope gradient was classified into five classes (<15°, 15°–25°, 25°–35°, 35°–45°, and >45° for GIS analysis.)

• Elevation: This map was also generated from the DEM, which can be used to classify the local relief and locate points of maximum and minimum heights. A contour map with 400 m elevation intervals was generated and analyzed.

• Distance from streams: This map was made by applying a buffer to the stream network, and was divided into five classes (<200 m, 200–400 m,400–600 m, 600–800 m, and >800 m from the streams).The hypothesis investigated whether or not there was a higher landslide frequency along streams, due to undercutting.

A Geographical Information System (GIS) database with different layers or coverages was compiled. All maps were stored in raster format with a pixel size of 20 m. All susceptibility factor maps were combined along with the landslide inventory map (Fig. 3) to calculate the positive and negative weights.

2.3 Landslide inventory

Landslide inventory and mapping are aimed at determining the processes involved in landslide development in the study area and the corresponding terrain instability factors. The landslide inventory and map in the study area were created using the following procedures:

(a) Field investigation: the landslide map was checked and corrected to obtain a definitive landslide map at 1:50,000 scale, and field observations were made in areas with the highest density of landslides to obtain information about the mechanisms and instability factors involved in terrain-failures;

(b) Aerial photograph interpretation: aerial photographs taken on May 20, 2008 were enlarged at 10,000 scale yielding an acceptable resolution and allowing a more detailed interpretation; and

(c) Landslide map digitalization: in the generated digital landslide map, the landslide locations and dimensions are provided (Fig. 3). Different landslide types were summarized in terms of the following classes: rockfalls (including rock falls, debris falls and

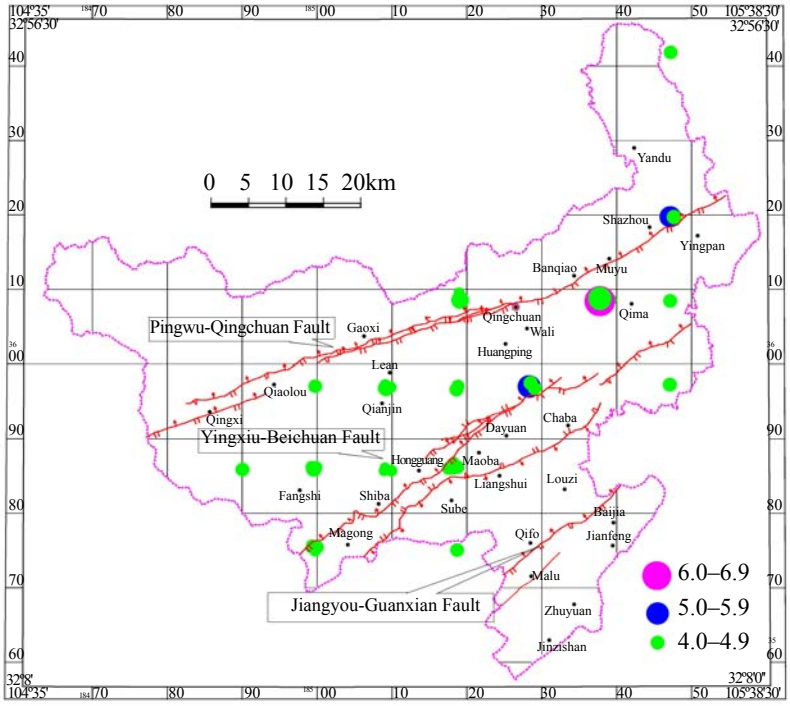

Fig. 2 Map showing faults and aftershock distribution in the study area

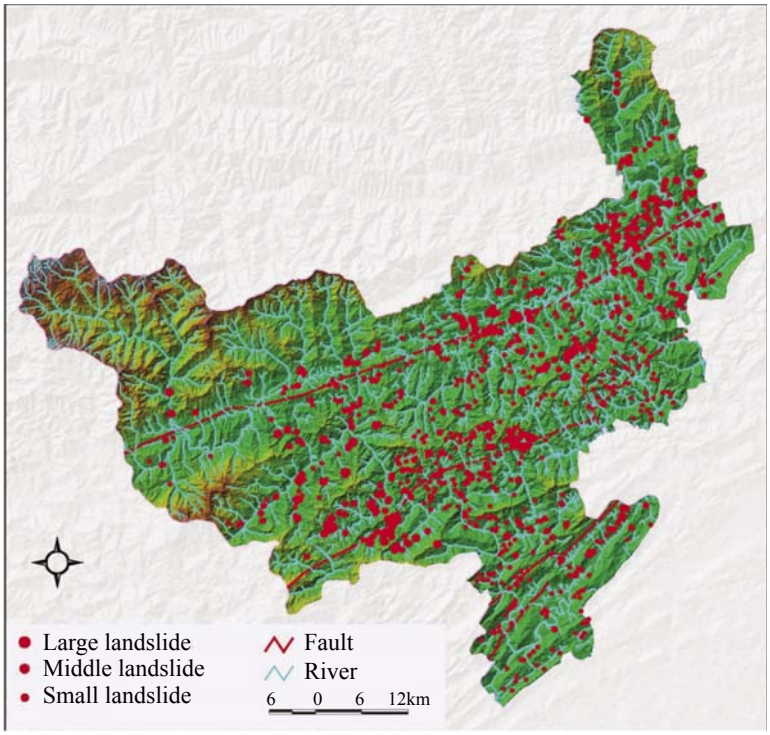

Fig. 3 Digital elevation model of the Qingchuan area; landslides triggered by the Wenchuan earthquake

rock avalanches); landslides (debris slides and rotational slides, slump); and debris flows, according to Varnes's classification (Varnes, 1984).

Post-earthquake field investigations and interpretation of aerial photographs throughout an area of 3271 km^2 were conducted immediately following the earthquake and about 971 earthquake-triggered landslides (see Figs. 4 & 5) were identified; most were called potential landslides, which were still hanging on the slope-walls and would fail further if a heavy rainfall were to occur. Each of the majority of the identified landslides has a volume of more than 1,000 m^3, and each of the forty large landslides has a volume of more than one million cubic meters. Three landslides, i.e., the Donghekou, Shibangou and Magong landslides, were catastrophic and were responsible for most of the loss of lives by landslides in Qingchuan County. More than several thousand smaller landslides were not recorded. The Wenchuan earthquake event-based landslide inventory is shown in Fig. 3.

2.4 Selection of susceptibility factors

Landslide occurrence in an earthquake affected area is a function of direct and indirect natural and human factors. These factors include, for example, lithology, structure, tectonics, geomorphology, topography, precipitation, temperature, infiltration, runoff, land cover, and road construction (Kamp *et al.*, 2008). A simplified approach requires a selection of a limited number of key susceptibility factors. The factors are selected in accordance with subjective expert opinion and depend on a priori knowledge (Kamp *et al.*, 2008; Akgün and Bulut, 2007; Conoscenti *et al.*, 2008). In selecting susceptibility factors, a multi-criteria evaluation was applied to determine the significance of event-controlling parameters in triggering the landslides in the 2005 Kashmir earthquake region. The parameters

Fig. 4 The Donghekou landslide with a volume of 10 million m^3 travel distance of 3 km and form a barrier lake. This landslide buried four villages and claimed 260 death tolls

Fig. 5 Aerial photograph taken on May 18, 2008 shows the location of large landslides and barrier lakes in the southern part of Qingchuan County

included lithology, faults, slope gradient, slope aspect, elevation, landcover, rivers and roads, etc. (Kamp *et al*., 2008). While in their study of seismic landslides in the 2001 El Salvador earthquake, García-Rodríguez *et al*. (2008) considered the following seven parameters: lithology (bedrock and soil), elevation, slope gradient, slope aspect, terrain roughness, and land use. It is clear from these two case studies that susceptibility factors share some common attributes, such as slope gradient, lithology types, elevation, and land use. The selection of factors that are used in the susceptibility assessment is dependent on the type of landslide and terrain and the availability of existing data and resources. Field observations also contribute to the understanding of earthquake induced slope-failure mechanisms and their contributing factors. Based on field observations and available data, the susceptibility factors selected for this study are: topography, lithology, faults and stream proximity. These factors can be also applied to landslide susceptibility assessment in other seismic regions. As the present study only deals with landslide susceptibility and not landslide hazard, information on triggering factors, such as rainfall indicators, were not taken into account.

In a statistical approach, all landslide susceptibility factors that can be mapped are entered into a GIS database and converted from vector to raster maps. After this, an overlay is made of each factor map with the landslide inventory map. The susceptibility index of each factor for the landslide occurrence is calculated by comparing the numbers of landslides within the area occupied by the factor, with the number of landslides in the entire area.

2.5 Weighting landslide susceptibility

In this study, the analytical hierarchy process (AHP) method was adopted to weigh the landslide susceptibility because of its precision and easy implementation. (Saaty, 1980). The AHP method compares all factors and assigns values agreed upon by experts; then, a matrix is formed for multifactor comparison and judgment. The AHP applies a one-level weighting system developed by a collection of expert opinions; in this study, the expert opinions are the experience obtained during the field investigation of May, 2008.

The results of the pair-wise comparison matrix and the factor weights are shown in Table 1. Based on the results of the pair-wise comparison matrix, the weighting modulus for factors of landslide susceptibility was acquired and the weighting modulus of slope gradient, elevation, rock type, fault proximity, and stream proximity are 0.30, 0.10, 0.18, 0.13 and 0.29, respectively. These results support our observation in field work that slope gradient and stream proximity were the most influential event-controlling parameters for landslides in the earthquake affected regions.

Areas with proximity to streams showed remarkable slope erosive processes and mass movement, which, in turn, caused intense, superficial slope failure phenomena

Table 1 Comparative matrix of factors impacting landslide susceptibility

Attribute	Slope gradient	Elevation	Lithology	Fault proximity	Stream proximity	Factor weights
Slope gradient	1	3	2	3	5	0.30
Elevation	1/2	1	1/3	1/2	1/3	0.10
Lithology	1	1/2	1	1	2	0.18
Fault proximity	3	1/2	1/3	1	1/2	0.13
Stream proximity	1	4	2	3	1	0.29

in areas adjacent to drainage channels. This factor was also the instability hazard from high pore-water pressures in the very fragmented landslide deposits that make up the river banks following possible rapid drawdown.

2.6 Assessment model

Once maps representing major landslide susceptibility factor were established, a mapping approach was used to calculate the landslide susceptibility index, and classical overlay operations were used to produce a landslide susceptibility map. The mapping procedure included the following three steps:

First each factor class was reclassified to generate separate susceptibility maps based on calculation results from the Susceptibility Index. The susceptibility factors were then standardized in order to properly compare them. The values of each factor were converted into a number of classes, depending on the susceptibility Index. Every class was assigned a value of 1, 2 or 3 representing a low, moderate, or high susceptibility level, respectively.

The second step was to establish an assessment model to calculate the landslide susceptibility value. The integration of the various factors in a single susceptibility index was accomplished by a procedure based on their weighted linear sum as follows:

$$I_{\mathrm{LS}} = a_j X_{ij} \tag{1}$$

where:
I_{LS}: landslide susceptibility index (LSI)
a_j: weight of factor j
X_{ij}: weight of class i in factor j

The calculation model is expressed as the following equation

$$I_{\mathrm{LS}} = 0.30X_1 + 0.10X_2 + 0.18X_3 + 0.13X_4 + 0.29X_5 \tag{2}$$

where X_1, X_2, X_3, X_4 and X_5 denote weights to susceptibility factors of slope gradient, elevation, rock type, fault proximity and stream proximity, respectively.

The I_{LS} represents the relative susceptibility of a landslide occurrence. Therefore, the higher the index, the more susceptible the area is to landslide.

The third step is to overlay all susceptibility factor maps to calculate the cumulative value. The cumulative value represents the relative propensity of the terrain to landsliding in each land surface unit. Landslide susceptibility classes and mapping obtained for each land surface unit can be classified into several intervals to define different susceptibility classes. These can be used to classify the land surface into different susceptibility degree domains.

In this study, the GIS processing module was applied to the grid resolution with 20 m × 20 m for each digital map layer. The final mapping procedure was carried out using the ArcGIS spatial analysis module. Multiplying the digital map of five factors involved in the assessment by their corresponding weights, the susceptibility index of each grid unit was estimated by adopting an overlay tool of ArcGIS.

3 Analysis results

3.1 Susceptibility for each factor

The calculated landslide distributions in terms of three susceptibility levels for five landslide susceptibility factors are illustrated in Figs. 6 (a) through (e), respectively.

(1) Topography

As topography is one of the major factors in landslide susceptibility analysis, the generation of a digital representation of the surface elevation plays a significant role. The elevation in the study area ranges from a minimum of ~ 491 m ASL in some river beds to a maximum of ~3837 m ASL in the northwest part of the study area. 72.93% of the study area is at elevations lower than 1400 m ASL; but only a few areas are higher than 1800 m ASL(~12.65%) as shown in Table 2. Note that the correlation of landslide number with elevation shows that 97.8% of the landslides occurred at elevations below 1400 m ASL, and 61.5% of all landsliding was found at elevations below 1000 m ASL (Fig. 6(b)). Landsliding was very scarce at elevations above 1800 m ASL.

Slope gradient is an important component and a preparatory cause of landsliding. The GIS work shows

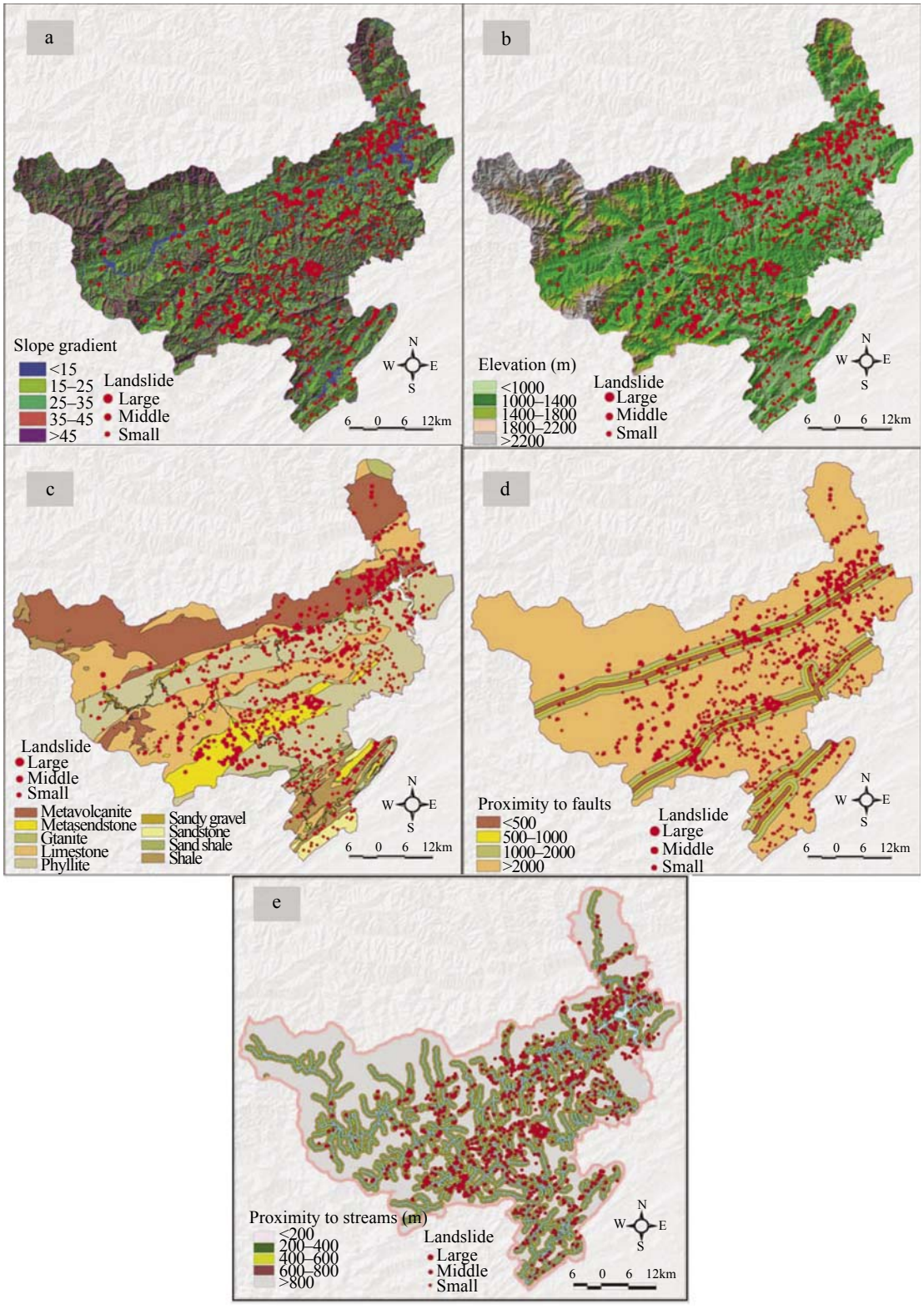

Fig. 6 Maps show the correlation of landslide distribution with slope gradiant (a), elevation (b), rock type (c), buffer zone for fault

that most of the landsliding occurred on slopes of 25–35°. Landsliding was not as frequent on very gentle (0–15°) and very steep (>45°) slopes, as shown in Table 3 and Fig. 6 (a).

(2) Lithology

In addition to topographic information, the second important type of environmental data for landslide susceptibility mapping is related to the materials

in which landslides might originate. Lithology is commonly considered to be one of the most important factors and is used in practically all works dealing with landslide susceptibility assessment. The analysis shows that most of the landslides occurred in highly fractured metasandstone, phyllite and shale. 14% of the landslides with 7% surface land in the study area occurred in metasandstone, which has the highest susceptibility index as indicated in Table 4. Large numbers (37%) of landslides occurred in phyllite, whereas, considerably fewer landslides occurred within granite, sandy gravel, and sandstone (see Fig. 6 (c)).

(3) Fault proximity

Three faults depicted on a 1:100 000 scale geological map were buffered at three intervals of 500 m (Fig. 6(d)). Generally, as the distance from the fault increases, landslide frequency decreases. The study showed that the susceptibility index of landslides increases with proximity to the fault lines (0.603 within the 500 m zone; 0.535 within the 500–1000 m zone; 0.425 within the 1000–2000 m zone and 0.239 beyond 2000 m zone). These results indicated that landsliding is more common with proximity to the active fault traces (Table 5). As in other studies (Leroi, 1996; Einstein, 1997; Tang, 2004; Western *et al.*, 2005), the distance to faults was used to classify the hazard. Within these zones, the bedrock is tectonically stressed and highly unstable. The smaller the distance to the fault, the higher the tectonic influence and the greater the index.

(4) Stream proximity

The extent of landslide susceptibility is closely related to its distance from streams. The buffered regions were rated according to their distance from major streams. In the GIS analysis, buffer zones for stream lines were set to <200, 200–400, 400–600, 600–800, and >800m (Table 6). The study showed that the susceptibility index of landslides increases with proximity to the stream lines (0.55 within the 200 m zone; 0.49 within the 200 – 400 m zone; 0.31 within the 400 – 600 m zone, 0.28 within the 600 – 800 m zone and 0.11 beyond 800 m zone). These results indicate that the shorter the distance, the higher the susceptibility index (see Fig. 6(e)). Table 5 shows the results of the analysis.

Each of the five factors was grouped into three categories, and each category was assigned a value between 1 and 3, with 1 being the least susceptible and 3 the most susceptible to landslides (Table 7).

3.2 Results of integrated assessment

An integration of these factors with certain weights and conditions yielded landslide susceptibility values. These values were integrated and assessed to create a landslide susceptibility map of the study area. The I_{LS}

Table 2 Relationship of landslides to elevation within the study area

Elevation (m)	< 1000	1000–1400	1400–1800	1800–2200	>2200
Area (km^2)	1198	1183	471	217	196
Area (%)	36.69	36.24	14.42	6.64	6.01
LS number	597	353	20	1	0
Susceptibility index	0.498	0.298	0.043	0.005	0

Table 3 Relationship of landslides to slope gradient within the study area

Slope (º)	<15	15–25	25–35	35–45	>45
Area (km^2)	362	653	1131	824	296
Area(%)	11.08	19.99	34.63	25.24	9.06
LS number	53	173	414	249	82
Susceptibility index	0.15	0.26	0.37	0.30	0.24

Table 4 Relationship of landslides to rock type within the study area

Lithology	Metavolcanite	Metasandstone	Granite	Limestone	Phyllite	Sandy Gravel	Sandstone	Sandshale	Shale
Area (km^2)	779	255	27	855	1043	48	55	50	153
Area (%)	23.03	7.8	0.82	26.2	31.94	1.48	1.69	1.52	4.69
LS number	111	134	5	246	388	9	14	25	39
Susceptibility index	0.143	0.526	0.185	0.287	0.372	0.188	0.254	0.500	0.255

is classified into three susceptibility categories: low, moderate and high. The I_{LS} value, susceptibility area and its ratio to the total susceptibility area for each susceptibility category are summarized in Table 8.

A comparison of the susceptibility map and event-triggered landslides illustrated in Fig. 7 shows a similar pattern of correspondence between landslides and high susceptibility (Fig. 3).

Based on the I_{LS} grid, there are three areas in Qingchuan County where a relatively high potential for landslides exists. Areas identified as having high landslide susceptibility were located in the central, northeastern, and far south regions of the study area (Fig. 7). The relatively high landslide potential of these areas is apparent due to unfavorable combinations of different factors.

3.3 Verification

To verify the seismic landslide susceptibility map in the Qingchuan area, the above method is applied to assess the susceptibility of the landslides in Beichuan County triggered by the Wenchuan earthquake. The Beichuan area is situated in the central part of the area affected by the earthquake. During the post-earthquake field investigation and interpretation of aerial photographs of the study area of 2,865 km^2 in Beichuan area, a total of 1,754 earthquake-triggered landslides were identified. The seismic landslide susceptibility map of Beichuan area is shown in Fig. 8. Comparing it to the seismic landslide inventory map in the Beichuan area, it is seen that about 88% of the coseismic landslides occurred in areas which were classified as "high" in the susceptibility map. It is concluded that the two maps (Fig. 7 and Fig. 8) have a similar pattern of correspondence between landslides and high susceptibility. The verification results show a satisfactory agreement between the susceptibility and the seismic landslide location data in the Beichuan area. Thus, the landslide susceptibility analysis results were reasonable and acceptable.

4 Conclusions

The seismic landslide susceptibility map was

Table 5 Relationship of landslides to fault proximity within the study area

Proximity to fault (m)	<500	500–1000	1000–2000	>2000
Area (km^2)	189	185	365	2526
Area (%)	5.79	5.67	11.18	77.37
LS number	82	89	153	647
Susceptibility index	0.434	0.481	0.419	0.256

Table 6 Relationship of landslides to stream proximity within the study area

Proximity to stream(m)	< 200	200–400	400–600	600-800	>800
Area (km^2)	578	508	439	364	1385
Area (%)	17.65	15.51	13.4	11.11	42.29
LS number	321	251	138	104	157
Susceptibility index	0.55	0.49	0.31	0.28	0.11

Table 7 Categories and rating for the five factors

Slope gradient (°)		Elevation (m)		Lithology		Fault proximity (m)		Stream proximity (m)	
Category	Rating	Category	Rating	Category	Rating	Category	Rating	Category	Rating
25-45	3	< 1000	3	Metasandstone Sandshale Phyllite	3	500-1000	3	< 400	3
15-25 >45	2	1000-1400	2	Limestone Sandstone Shale	2	< 500 1000-2000	2	400-800	2
<15	1	> 1400	1	Sandy Gravel Metavolcanite Granite	1	> 2000	1	>800	1

Table 8 Results of characteristics from seismic landslide susceptibility assessment for the study area

Susceptibility categories	I_{LS}	Susceptibility	
		Area (km^2)	Ratio (%)
Low	1.00 – 1.50	1063.1	32.5
Moderate	1.51 – 2.00	837.3	25.6
High	2.01 – 3.00	1370.6	41.9

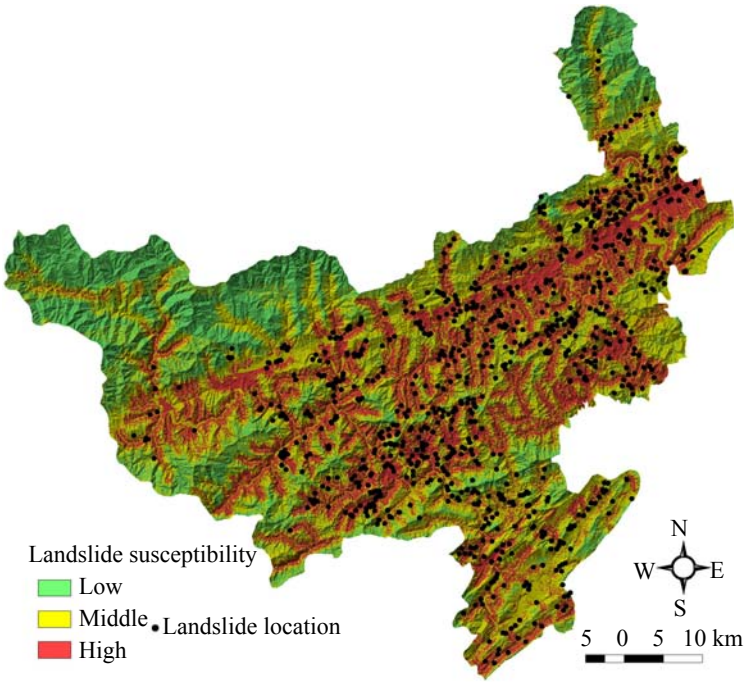

Fig. 7 Seismic landslide susceptibility assessment of the study area

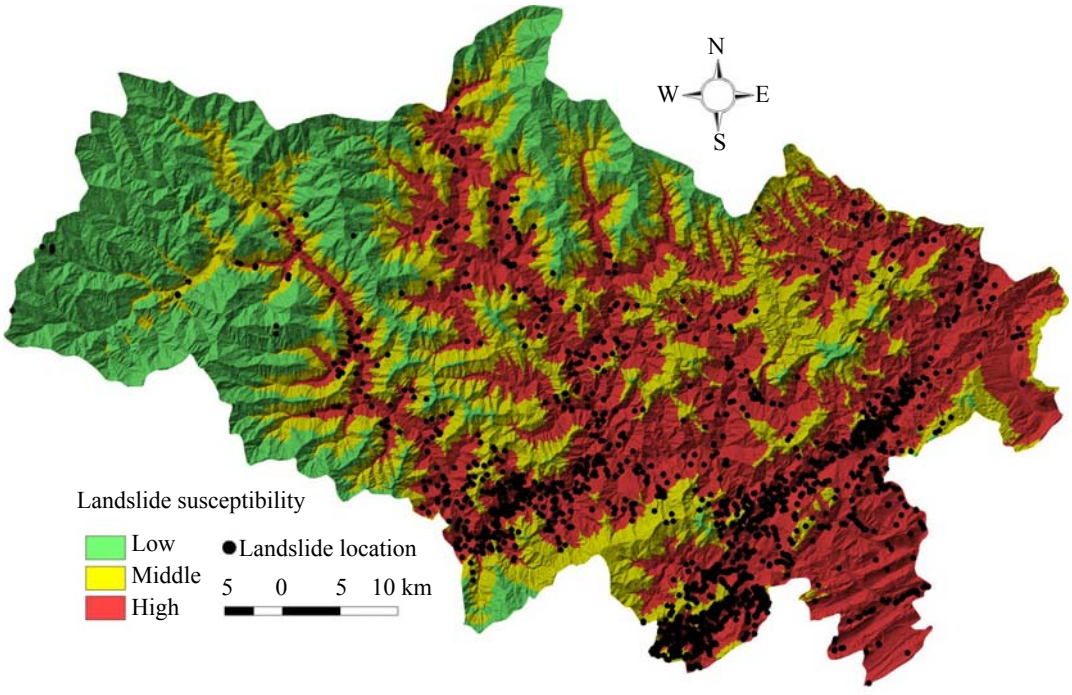

Fig. 8 Seismic landslide susceptibility assessment in the Beichuan area for verification

produced in a short period of time based on limited data sources following an emergency request made after the earthquake. A pilot study area was selected in Qingchuan County. This study was carried out to determine which factors were likely to cause landslides and describes the approach used to assess landslide susceptibility in the earthquake affected area. A numerical rating system was applied to five factors that may have contributed to the occurrence of the Wenchuan earthquake-triggered landslides. From the results, some major conclusions are as follows:

(1) Lithology, slope angle, streams and faults are important event-controlling factors for landslide susceptibility mapping. The map shows landslide susceptibility is highly controlled by the Longmenshan fault zone as well as topography, rock type, and stream proximity.

(2) Areas identified as having high landslide susceptibility were located in the central, northeastern, and far south regions of the study area. Each of these areas has different combinations of factors leading to a relatively high landslide potential.

(3) This landslide-susceptibility map appears to be a satisfactory predictor of future landslide activity, which can be provided to planners for site selection and site-planning for post-earthquake reconstruction activities. The maps may also be used as a basis for landslide risk management in the study area.

(4) The methods for emergency landslide susceptibility mapping have been verified to be effective for rapid response to earthquake induced landslide analysis via our practice of emergency mapping after the massive Wenchuan earthquake.

Landslide susceptibility should be a primary consideration in reconstruction planning after the Wenchuan earthquake. Additionally, planners could use the landslide susceptibility map to identify roads and facilities that can potentially be damaged by future landslide activity.

Note that in addition to earthquakes, heavy rain can also be a triggering factor for landslides (Westen *et al.*, 2005). In our work, the landslide susceptibility assessment was performed based on an inventory of landslides caused by the 2008 Wenchuan earthquake, without considering the effect of heavy rain. This also explains the difference between our results and those of the previous studies. In future studies, it will be necessary to develop a model of landslide susceptibility that incorporates rainfall.

Acknowledgement

This research was developed within the framework of the emergency projects financed by the Sichuan Department of Land and Resources, 973 Program (2008CB425801), Research Foundation of SKLGP and the National Foundation for Natural Science of China (40772206). Cartographic data were provided by the Sichuan Department of Land and Resources. The authors wish to express their sincere thanks for these contributions, in particular Prof. Niek Rengers and Dr. C.J. van Westen from International Institute for Geo-Information Science and Earth Observation in Netherlands (ITC) for their many suggestions on this study.

References

Akgün A and Bulut F (2007), "GIS-based Landslide Susceptibility for Arsin-yomra (Trabzon, North Turkey) Region," *Environmental Geology*, **51**: 1377–1387.

Conoscenti C, Di Maggio C and Rotiglinao E (2008), "GIS Analysis to Assess Landslide Susceptibility in a Fluvial Basin of NW Sicily (Italy)," *Geomorphology*, **94**: 325–339.

Einstein HH (1997), "Landslide Risk-systematic Approaches to Assessment and Management," Cruden DM and Fell R, *landslide Risk Assessment*, Rotterdam: A.A.Balkema, pp. 51-109.

García-Rodríguez MJ, Malpica JA, Benito B and Díaz M (2008), "Susceptibility Assessment of Earthquake-Triggered Landslides in El Salvador Using Logistic Regression," *Geomorphology*, **95**:172–191.

Kamp U, Growley BJ and Khattak GA (2008), "GIS-Based Landslide Susceptibility Mapping for the 2005 Kashmir Earthquake Region," *Geomorphology*, **101**: 631–642.

Leroi E (1996), "Landslide Hazard-risk Maps at Different Scales: Objectives, Tools and Development," *Proc. Seventh International Symposium on Landslide*s, Trondheim, Norway, pp. 35–52.

Saaty TL (1980), *The Analytical Hierarchy Process*, New York: McGraw-Hill.

Tang C (2004), "A Study on Landslide Risk Mapping," *Journal of Natural Disasters*, **13**(3): 8–12. (in Chinese)

Westen CJ, Van Asch TWJ and Soeters R (2005), "Landslide Hazard and Risk Zonation; Why Is It Still So Difficult?" *Bulletin of Engineering Geology and the Environment*, the Official Journal of the International Association for Engineering Geology and the Environment : (IAEG), **65**(2): 167–184.

Varnes DJ (1984), *Landslide Hazard Zonation: A Review of Principles and Practice*. Paris: United Nations International.

Yin Y (2009), "Features of Landslides Triggered by the Wenchuan Earthquake," *Journal of Engineering Geology*, **17**(1): 29–38. (in Chinese)